NUWC-NPT Technical Report 11,011
17 October 1995

An Analytical Solution for the Unsteady Flow of a Bingham Plastic Fluid in a Circular Tube

Stephen A. Austin
Submarine Sonar Department

Naval Undersea Warfare Center Division
Newport, Rhode Island

PREFACE

The research in this report was developed by Dr. S. A. Austin of the Naval Undersea Warfare Center (NUWC), Detachment New London (Code 2141), under the NUWC Division Newport Independent Research (IR) Program, Project Number B10004, *Detection and Localization of Internal Acoustic Emissions in a Three-Dimensional Structure*, principal investigator Dr. A. J. Hull (Code 2141). The IR program is funded by the Office of Naval Research; the NUWC Division Newport program manager is Dr. S. C. Dickinson (Code 102).

The technical reviewer for this report was B. M. Abraham (Code 2141).

The author wishes to thank K. A. Holt for her help with the editing of the manuscript.

Reviewed and Approved: 17 October 1995

R. J. Martin
Acting Head, Submarine Sonar Department

REPORT DOCUMENTATION PAGE

Form Approved
OMB No. 0704-0188

1. AGENCY USE ONLY (Leave Blank)	2. REPORT DATE	3. REPORT TYPE AND DATES COVERED
	17 October 1995	Final

4. TITLE AND SUBTITLE

An Analytical Solution for the Unsteady Flow of a Bingham Plastic Fluid in a Circular Tube

5. FUNDING NUMBERS

6. AUTHOR(S)

Dr. Stephen A. Austin

7. PERFORMING ORGANIZATION NAME(S) AND ADDRESS(ES)

Naval Undersea Warfare Center
Detachment New London
New London, Connecticut 06320

8. PERFORMING ORGANIZATION REPORT NUMBER

TR 11,011

9. SPONSORING/MONITORING AGENCY NAME(S) AND ADDRESS(ES)

10. SPONSORING/MONITORING AGENCY REPORT NUMBER

11. SUPPLEMENTARY NOTES

12a. DISTRIBUTION/AVAILABILITY STATEMENT

Approved for public release; distribution is unlimited.

12b. DISTRIBUTION CODE

13. ABSTRACT (Maximum 200 words)

This report describes a closed form solution of the axial velocity profile and the shear stress profile for a Bingham plastic fluid in a circular tube. The analysis simulates the commencement of flow resulting from a pressure gradient. Past numerical and analytical solutions are shown to be deficient in the early stages of the flow when they are compared with the closed form solution presented here.

14. SUBJECT TERM

Axial Velocity Profile, Bingham Plastic Fluid, Closed Form Solution, Non-Newtonian Fluid Model, Shear Stress Profile, Unsteady Fluid Flow

15. NUMBER OF PAGES

36

16. PRICE CODE

17. SECURITY CLASSIFICATION OF REPORT	18. SECURITY CLASSIFICATION OF THIS PAGE	19. SECURITY CLASSIFICATION OF ABSTRACT	20. LIMITATION OF ABSTRACT
UNCLASSIFIED	UNCLASSIFIED	UNCLASSIFIED	SAR

TABLE OF CONTENTS

LIST OF ILLUSTRATIONS

LIST OF ILLUSTRATIONS (CONT'D)

LIST OF TABLES

AN ANALYTICAL SOLUTION FOR THE UNSTEADY FLOW OF A BINGHAM PLASTIC FLUID IN A CIRCULAR TUBE

1. INTRODUCTION

The solution of unsteady, non-Newtonian fluid velocity profiles is developed using numerical approximations as found in Edwards et al. (1972), Lipscomb and Denn (1984), Duggins (1972), Atkin et al. (1991), and Walton and Bittleston (1991). The closed form solution of unsteady velocity profiles in circular tubes has been accomplished by Szymanski (1932) for Newtonian fluids. An attempt to provide a closed form solution of the unsteady flow in circular tubes was made by Atabek (1964) for a non-Newtonian Bingham plastic fluid. The predominant method of solution for a Bingham plastic fluid in a circular tube has been to assume the form of the velocity profile in the boundary layer region, which was done by Chen et al. (1970) with an integral equation-based solution and by Duggins (1972) with a numerical solution.

In this report, the solution of the start-up of a Bingham flow in a long circular tube is presented in an analytical closed form. This non-Newtonian fluid model will be compared with Newtonian fluid models in order to determine the rheological influence for such borderline fluids as blood, which exhibit characteristics of both fluid classifications.

2. SYSTEM MODEL

The governing equations for a Bingham fluid within a long circular tube are developed from the Cauchy formulation of the momentum equations. Since the cylinder is considered long, compared to the radius, the velocity profile inside the tube is assumed to be in the axial direction. The momentum equation in the axial direction is expressed for a general fluid as (Bird et al. (1960))

$$\rho\frac{Du}{Dt} = -\frac{\partial P}{\partial z} - \left(\frac{1}{r}\frac{\partial}{\partial r}(r\tau_{rz}) + \frac{1}{r}\frac{\partial \tau_{\theta z}}{\partial \theta} + \frac{\partial \tau_{zz}}{\partial z}\right) + \rho g_z \ , \qquad (1)$$

where D/Dt is the substantial derivative, u is the axial component of velocity (m/s), P is the fluid pressure field (Pa), τ_{rz} is the shear stress acting on the radial face in the axial direction (Pa), $\tau_{\theta z}$ is the shear stress acting on the circumferential face in the axial direction (Pa), τ_{zz} is the normal longitudinal stress on the fluid (Pa), ρ is the fluid mass density (kg/m^3), g_z is the axial component of gravitational acceleration (m/s^2), r is the radial coordinate (m), θ is the circumferential coordinate (radians), z is the axial coordinate (m), and t is time (s). The fluid flow applications of interest are those assumed for a horizontal tube ($g_z = 0$) that is axisymmetric. The remaining spatial parameters, after applying this assumption, are the radius of the tube and the axial location along the tube. The expression of the momentum in the axial direction in terms of the fluid velocity is obtained by substituting the Bingham constitutive relationship into equation (1) for the stress components, which is found in Bird et al. (1960) to be

$$\tau_{rz} = \tau_0 - \mu \frac{\partial u}{\partial r} \tag{2}$$

when the shear stress is equal to or greater than the yield stress of the fluid, τ_0. The Newtonian component in equation (2) contains the absolute viscosity, μ, of the fluid (Pa-s) and the rate of shear strain (1/s) in terms of the spatial velocity gradient. When the shear stress is less than the yield shear stress of the fluid, the flow is considered plugged.

Since this analysis governs an axisymmetric cylindrical tube for a one-dimensional flow, the normal stresses and the radial component of velocity vanish from equation (1). Based on the one-dimensional flow assumption and the symmetry of the problem, the continuity equation becomes

$$\frac{\partial u}{\partial z} = 0 \ . \tag{3}$$

The axial velocity of the fluid is a function of time, t, and the radial coordinate, r. The effect of the one-dimensional flow assumption and the symmetry of the problem reduces the momentum equations in the radial and circumferential directions to

$$\frac{\partial P}{\partial r} = 0 \tag{4}$$

and

$$\frac{\partial P}{\partial \theta} = 0. \tag{5}$$

The substitution of equation (2) into equation (1) produces a momentum equation in the axial direction in terms of the axial velocity and the pressure gradient in the axial direction driving the flow. The implication of equations (4) and (5) result in the pressure being a function of only the axial location, which is consistent with the boundary layer theory assumptions. The governing equation for the unsteady flow of a Bingham fluid in a long circular tube thus becomes

$$\rho\frac{\partial u}{\partial t} = -\frac{dP}{dz} + \mu\frac{1}{r}\frac{\partial}{\partial r}(r\frac{\partial u}{\partial r}) - \frac{\tau_0}{r}. \tag{6}$$

The spatial domain governed by equation (6) is represented in figure 1. The radial domain extends from zero, at the center of the tube, to the inside radius, a. The axial domain extends from zero to the final length, l, of the tube. The solution to the axial velocity governed by equation (6) is valid for a completely filled cylinder only. This region is represented at an axial location greater than (Bird et al., 1960)

$$0.26\frac{u_{max}a^2}{\nu}, \tag{7}$$

where ν is the kinematic viscosity of the fluid (m^2/s) and u_{max} is the maximum axial velocity of the flow. The location of the flow region shown here is valid for laminar flow applications. The boundary conditions consist of zero velocity on the tube wall and a finite velocity at the center of the tube when the radius goes to zero. The initial condition requires the fluid to be at rest.

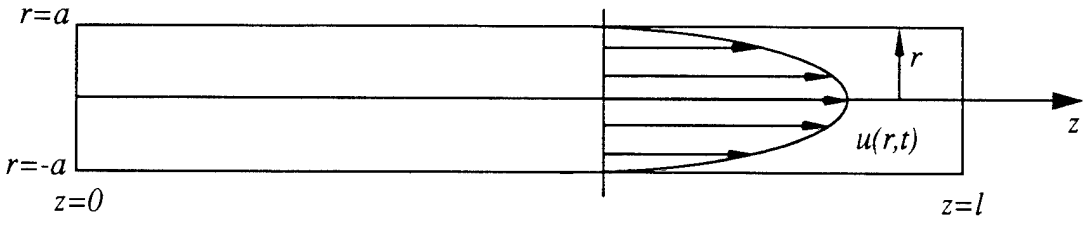

Figure 1. Flow Domain

Since the pressure is only dependent on the axial coordinate, the gradient can be represented as the difference between the entrance and exit pressure divided by the length of the circular tube. The analysis is conducted by nondimensionalizing equation (6). The parameters used to nondimensionalize the governing equation are

$$\Phi = \frac{4\mu l u(r,t)}{a^2 (P_0 - P_l)}, \qquad \xi = \frac{r}{a}, \qquad \sigma = \frac{\mu t}{\rho a^2}, \tag{8}$$

where $\Phi(\xi,\sigma)$ is the nondimensional axial velocity, ξ is the nondimensional radial coordinate, and σ is nondimensional time. The substitution of the parameters in equation (8) into equation (6) produces the unsteady flow of a Bingham plastic fluid in a circular tube as

$$\frac{\partial \Phi}{\partial \sigma} = 4 + \frac{1}{\xi}\frac{\partial}{\partial \xi}\left(\xi \frac{\partial \Phi}{\partial \xi}\right) - \frac{\alpha}{\xi} \quad , \tag{9}$$

with

$$\alpha = \frac{4l\tau_0}{a\,(P_0 - P_l)} . \tag{10}$$

The nondimensionalized boundary conditions and the initial condition have the following form:

$$\begin{aligned} &\sigma = 0, time = 0 \qquad \Phi = 0 \\ &\xi = 1, radius = a \qquad \Phi = 0 \\ &\xi = 0, radius = 0 \qquad \Phi \rightarrow finite \, . \end{aligned} \tag{11}$$

The form of equation (9) as presented is not separable for direct solution. In order to obtain a separable form, the nondimensional axial velocity will be assumed to have the form

$$\Phi(\xi, \sigma) = \Phi_\infty(\xi) - \Phi_\sigma(\xi, \sigma) , \tag{12}$$

where $\Phi_\infty(\xi)$ is the steady state solution when nondimensional time goes to infinity and $\Phi_\sigma(\xi, \sigma)$ is the unsteady portion of the total solution. The steady state solution is obtained first by substituting $\Phi_\infty(\xi)$ into equation (9); next by integrating the resulting ordinary differential with respect to the radial direction, as shown in equation (13),

$$\alpha - 4\xi = \frac{d}{d\xi}\left(\xi \frac{d\Phi_\infty}{d\xi}\right); \tag{13}$$

and finally by applying the boundary conditions of equation (11). The steady state portion of the total solution expressed by equation (12) becomes

$$\Phi_\infty(\xi) = \xi(\alpha - \xi) - \alpha + 1. \tag{14}$$

The substitution of equation (14) into equation (12) produces the foundation for the unsteady solution to the differential equation (9) as

$$\Phi(\xi, \sigma) = \xi(\alpha - \xi) - \alpha + 1 + \Phi_\sigma(\xi, \sigma) . \tag{15}$$

By taking the partial derivatives with respect to time and axial location in equation (15) and placing these terms into equation (9), an unsteady, separable partial differential equation is developed:

$$\frac{\partial \Phi_\sigma}{\partial \sigma} = \frac{1}{\xi}\frac{\partial}{\partial \xi}\left(\xi \frac{\partial \Phi_\sigma}{\partial \xi}\right). \tag{16}$$

The initial condition and the boundary conditions transform as follows:

$$\begin{aligned} \sigma &= 0 \qquad \Phi_\sigma = \Phi_\infty \\ \xi &= 1 \qquad \Phi_\sigma = 0 \\ \xi &= 0 \qquad \Phi_\sigma \rightarrow finite . \end{aligned} \tag{17}$$

The assumed solution for the unsteady problem, equation (16), is dependent on two functions: the nondimensional time and the nondimensional axial location:

$$\Phi_{\sigma}(\xi, \sigma) = \psi(\xi)\chi(\sigma) \ . \tag{18}$$

Substituting the proper partial derivatives of equation (18) into equation (16) results in the following separable differential equation:

$$\frac{1}{\chi}\frac{d\chi}{d\sigma} = \frac{1}{\psi\xi}\frac{d}{d\xi}(\xi\frac{d\psi}{d\xi}) = -\lambda^2, \tag{19}$$

where λ^2 is the separation constant. Based on this assumed solution, the ordinary differential equations in equation (19) can be separated into the following two ordinary differential equations:

In terms of nondimensional time,

$$\frac{d\chi}{d\sigma} + \lambda^2\chi = 0 \ , \tag{20}$$

In terms of nondimensional space,

$$\frac{1}{\xi}\frac{d}{d\xi}(\xi\frac{d\psi}{d\xi}) + \lambda^2\psi = 0 \ . \tag{21}$$

The resulting ordinary differential equations are found to be the Helmholtz differential equation (equation (20)) and a zero-order Bessel equation (equation (21)). The general form of solution for these differential equations is

$$\chi(\sigma) = C_1 e^{-\lambda^2 \sigma} \tag{22}$$

for the dependence on nondimensional time. The spatial dependence portion of the solution becomes

$$\psi(\xi) = C_2 J_0(\lambda\xi) + C_3 Y_0(\lambda\xi), \tag{23}$$

where C_1, C_2, and C_3 are arbitrary constants resolved by the initial condition and boundary conditions; J_0 is the zero-order Bessel function of the first kind; Y_0 is the zero-order Bessel function of the second kind; and λ is the appropriate separation constant.

The application of the boundary conditions (equation (17) to equation (23)) produces

$$\psi(\xi) = \sum_{n=1}^{\infty} D_n J_0(\lambda_n \xi), \tag{24}$$

where λ_n are the nth zeroes of the Bessel function of the first kind and D_n is an arbitrary constant. The combination of equations (22) and (24) develops the total solution of the unsteady flow of the Bingham fluid in a circular tube:

$$\Phi_\sigma(\xi, \sigma) = \sum_{n=1}^{\infty} B_n e^{-\lambda_n^2 \sigma} J_0(\lambda_n \xi) \ . \tag{25}$$

The arbitrary constant, B_n, is the combination of the constants found in equations (22) and (24). Since the final solution is given as the difference between the steady state solution and the unsteady solution, the solution for the remaining constant, B_n, becomes

$$\alpha\xi - \xi^2 + 1 - \alpha = \sum_{n=1}^{\infty} B_n J_0(\lambda_n \xi) \, . \tag{26}$$

The solution of B_n is obtained through the orthogonalization of equation (26) by multiplying both sides by $J_0(\lambda_m \xi)\,\xi$ and integrating with respect to ξ from zero to one. Since Bessel functions are orthogonal, the only right-hand side representation that is nonvanishing is when $m = n$ as shown in

$$\int_0^1 J_0(\lambda_n \xi)\, \xi\, (\alpha\xi - \xi^2 + 1 - \alpha)\, d\xi = \int_0^1 B_n J_0(\lambda_n \xi)\, J_0(\lambda_n \xi)\, \xi d\xi \, . \tag{27}$$

The left-hand side integral in equation (27) cannot be entirely solved analytically (Potter (1978)). The simplest form for the constant B_n is expressed as

$$B_n = \frac{8}{\lambda_n^3 J_1(\lambda_n)} + 2\alpha \left[\frac{\beta_n}{J_1^2(\lambda_n)} - \frac{1}{\lambda_n J_1(\lambda_n)} \right], \tag{28}$$

with

$$\beta_n = \int_0^1 \xi^2 J_0(\lambda_n \xi)\, d\xi. \tag{29}$$

The nondimensionalized velocity for the unsteady flow of a Bingham fluid in a long circular tube is expressed by combining equations (14), (25), (28), and (29) into equation (12), producing

$$\Phi(\xi, \sigma) = (1-\xi^2) + \alpha(\xi - 1) - \sum_{n=1}^{\infty} \frac{J_0(\lambda_n \xi)}{J_1(\lambda_n)} \left\{ \frac{8}{\lambda_n^3} + 2\alpha \left[\frac{\beta_n}{J_1(\lambda_n)} - \frac{1}{\lambda_n} \right] \right\} e^{-\lambda_n^2 \sigma}. \tag{30}$$

The velocity model described by equation (30) should revert to the Newtonian solution found in Szymanski (1932) when the Bingham yield stress goes to zero. Therefore, α becomes zero and equation (30) represents the unsteady Newtonian solution

$$\Phi_{\alpha \to 0}(\xi, \sigma) = (1-\xi^2) - \sum_{n=1}^{\infty} \frac{J_0(\lambda_n \xi)}{J_1(\lambda_n)} \frac{8}{\lambda_n^3} e^{-\lambda_n^2 \sigma}. \tag{31}$$

In an additional check, the solution is bounded at the center of the tube ($\xi = 0$). Applying this value of ξ to equation (30) produces

$$\Phi(0, \sigma) = 1 - \alpha - \sum_{n=1}^{\infty} \frac{1}{J_1(\lambda_n)} \left\{ \frac{8}{\lambda_n^3} + 2\alpha \left[\frac{\beta_n}{J_1(\lambda_n)} - \frac{1}{\lambda_n} \right] \right\} e^{-\lambda_n^2 \sigma}. \tag{32}$$

The steady state solution at the center of the circular tube ($\sigma = \infty$) then becomes

$$\Phi(0,\infty) = 1-\alpha \quad . \tag{33}$$

The steady state solution for the center velocity of the circular tube becomes unity at the Newtonian limit ($\alpha \to 0$). This is the expected solution found in Szymanski (1932). The developed model describing the nondimensional velocity of the Bingham fluid satisfies the initial condition and the boundary conditions of the flow, and has been shown to revert to the Newtonian solution.

The nondimensional shear stress can be evaluated from the velocity profile provided by equation (30). The constitutive relationship used to relate the velocity gradient to the shear stress was found in equation (2) to be that of a Bingham plastic fluid. The resulting shear stress in equation (2) is nondimensionalized by the parameter

$$\tilde{\tau}(\xi,\sigma) = \frac{2l\tau_{rz}}{a(P_0-P_l)}. \tag{34}$$

This nondimensionalization is accomplished by dividing the shear stress by the steady state shear stress at the wall of the circular tube. The nondimensional shear stress developed in the yielded region of the flow is evaluated by

$$\tilde{\tau}(\xi,\sigma) = \xi - \sum_{n=1}^{\infty} \frac{\lambda_n J_1(\lambda_n \xi)}{J_1(\lambda_n)} \left\{ \frac{4}{\lambda_n^3} + \alpha \left[\frac{\beta_n}{J_1(\lambda_n)} - \frac{1}{\lambda_n} \right] \right\} e^{-\lambda_n^2 \sigma}. \tag{35}$$

The location of the unyielded region, or the plugged flow region, is calculated from the dynamic shear stress at the tube wall. The plugged flow region is located at the critical radius, ξ_0, which is

evaluated by taking the ratio of the fluid yield stress to the dynamic wall shear stress. At a radius greater than the critical radius, equation (30) for the velocity applies. When the radius is less than or equal to the critical radius, the flow is plugged and the velocity is constant across the radius of the tube with a magnitude defined by equation (30) evaluated at ξ_0. The regions of plugged and yielded flows are illustrated in figure 2 using a representative value of 0.4 for ξ_0. The ordinate represents the normalized axial velocity; the abscissa represents the normalized tube radius from the tube center to the tube wall.

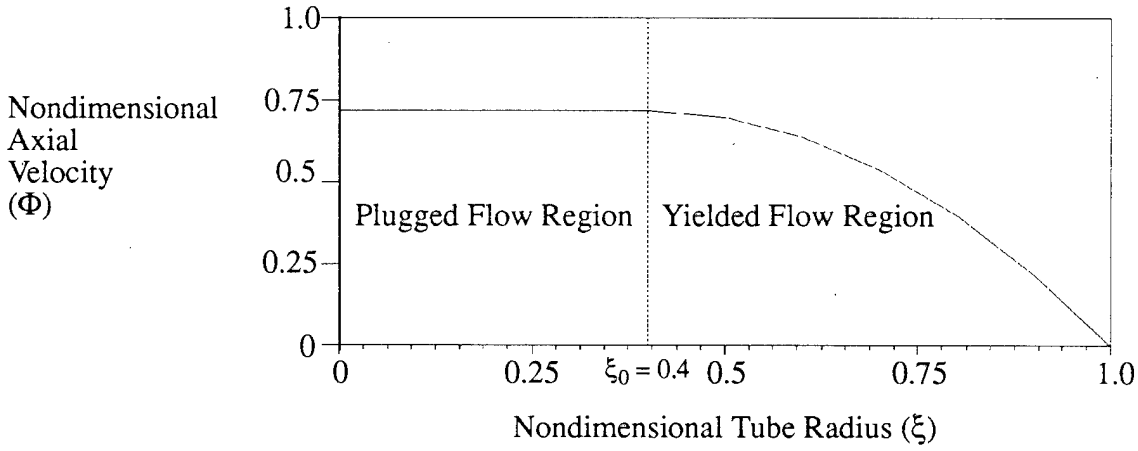

Figure 2. Plugged Flow and Yielded Flow Region Locations

3. MODEL VALIDATION

The axial velocity model for the Bingham plastic fluid developed in equation (30) is compared to the steady state solution found in Churchill (1988). In order to compare the steady state solution of Churchill to that of the converged steady state solution of equation (30), the velocity profile must be divided by the average velocity. The average velocity is the ratio of the integral of the velocity over the area to the cross-sectional area of the tube. The plugged flow region and the yielded flow region are integrated separately over the radius. The above mathematical operations result in equation (36):

$$\Phi_{ave} = \overbrace{\left[\frac{1}{6}(\xi_0)^4 - \frac{2}{3}(\xi_0) + \frac{1}{2}\right]}^{\text{Steady State Solution}} \underbrace{-I_{Bessel} - \frac{1}{2}\sum_{n=1}^{\infty} \Upsilon_n J_0(\lambda_n \xi_0)\,\xi_0^2}_{\text{Transient Solution}}, \tag{36}$$

with

$$I_{Bessel} = \int_{\xi_0}^{1} \sum_{n=1}^{\infty} \Upsilon_n \xi J_0(\lambda_n \xi)\, d\xi \tag{37}$$

and

$$\Upsilon_n = \frac{1}{J_1(\lambda_n)}\left[\frac{8}{\lambda_n^3} + 2\alpha\left[\frac{\beta_n}{J_1(\lambda_n)} - \frac{1}{\lambda_n}\right]\right] e^{-\lambda_n^2 \sigma}. \tag{38}$$

The normalized axial velocity is calculated by dividing the axial velocity in equation (30) by the average velocity expressed in equation (36). This result is compared to the steady state Bingham flow in a round tube given by Churchill (1988) (see figure 3). The ordinate in the figure represents the normalized axial velocity, and the abscissa represents the nondimensional radius of the round tube. This analysis shows a curious result: $\Phi/\Phi_{ave} = 1$ when the critical radius, ξ_0, is equal to one. Physically this represents the condition where the yield shear stress of the Bingham fluid is equal to the wall shear stress. Since the resistive shear stress in the fluid (τ_0) and the driving shear

stress (τ_w) are equal, no fluid flow should occur. The plugged flow condition exists across the complete tube; therefore, the expected solution would be zero fluid velocity. However, when the velocity is calculated for this case, the undefined expression of zero over zero is obtained. The evaluation of this limiting case is done by performing a L' Hopital operation on the normalized velocity, which calculates the result as one.

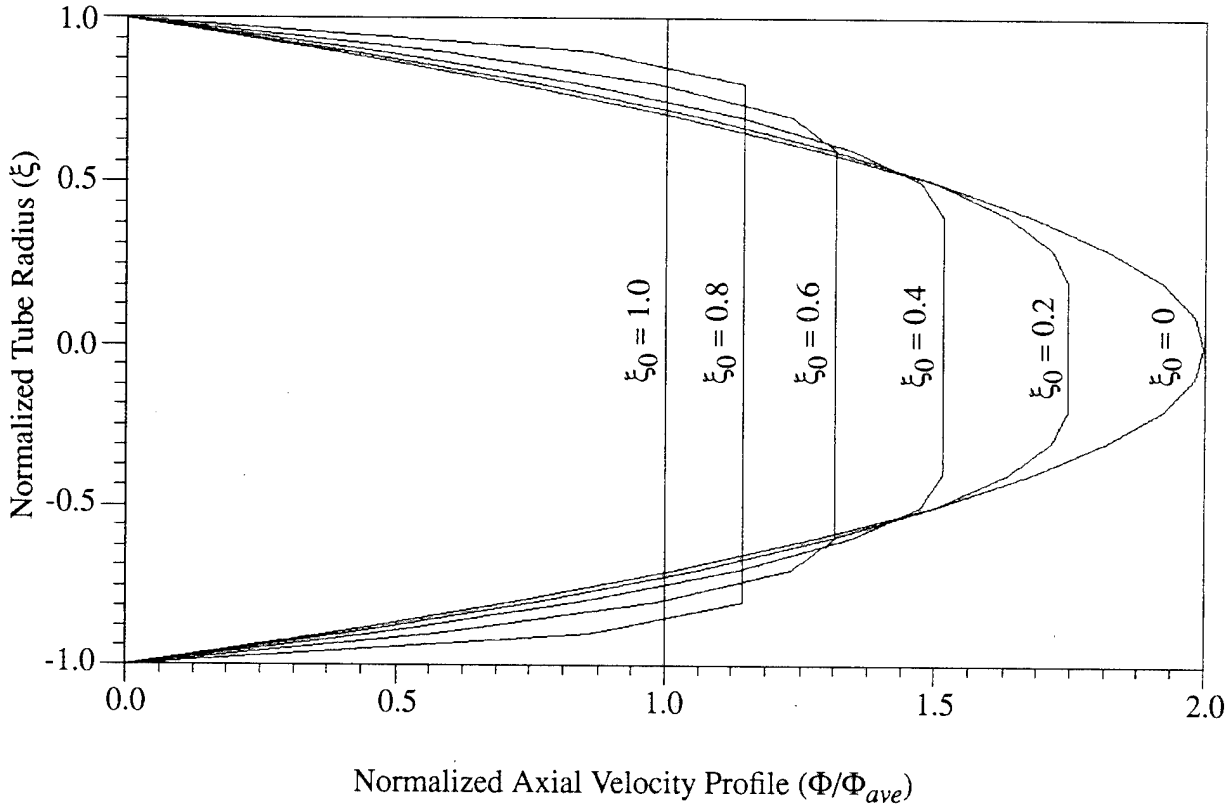

Figure 3. Velocity Profile for Steady State Laminar Flow of Various Bingham Fluids in a Circular Tube

The limiting case of a Newtonian fluid, $\xi_0 = 0$, is also shown in figure 3, with the characteristic Poiseuille velocity profile. As the rheological resistance to the fluid flow decreases, the region of the yielded fluid increases. Likewise, the region of plugged flow decreases as the yield shear stress decreases.

4. ANALYSIS

The parameter needed to resolve the normalized axial velocity and the normalized shear stress is the ratio of the fluid yield shear stress to that of the tube wall shear stress. In order to compare the results of the closed form analytical model presented here to the numerical approximation of Duggins (1972), a ratio of 0.25 is used. The prediction of the fluid velocity in the work of Duggins requires the assumption that the velocity profile is parabolic for the first two nodal locations from the wall of the tube. Applying this assumption to the velocity profile near the wall provides excellent agreement with the steady state solution. However, the evaluation of the transient fluid velocity has errors greater than 10 percent for 87 percent of the solution. The comparison of the velocity ratio between the maximum velocity to the average velocity for the closed form solution and the solution of Duggins is shown in table 1.

Table 1. Comparison of Duggins (1972) Approximation and the Closed Form Solution of the Commencement of Flow for a Bingham Fluid

Time (nondim.)	Φ_{max}/Φ_{ave} Duggins	Φ_{max}/Φ_{ave} Closed Form	Difference % Δ	% Steady State Solution
0.0513	1.335	0.639	109.0	38.0
0.1014	1.458	0.937	56.0	56.0
0.1510	1.531	1.136	35.0	67.5
0.2002	1.578	1.280	23.0	76.0
0.2995	1.631	1.464	11.0	87.0
0.4007	1.656	1.564	5.9	93.0
0.5034	1.669	1.619	3.0	96.0
0.7520	1.681	1.669	0.7	99.0
1.0	1.6835	1.6806	0.2	99.8
1000.0	1.6842	1.6842	0.0	100.0

The solution to the evolution of fluid flow in the circular tube approaches the steady state condition rapidly. The numerical approximation of Duggins (1972) produces extreme errors for

the transient solution and approaches accurate values only after the transients have decayed. Therefore, this numerical solution becomes valid for the steady state problem, as shown in the table. The interesting aspect of the transient solution is the nonlinearity of the shear stress profiles that are produced in the closed form solution. These shear stress profiles are important in the estimation of the energy dissipation by the viscous fluid forces.

The only known attempt to analytically solve the start-up flow of a Bingham plastic fluid is that of Atabek (1964). This solution appears to have the transient portion of the Bingham plastic fluid in addition to the steady state solution form, as shown in equations (30) and (35). However, on closer inspection of Atabek's solution, the transient terms are simply the Newtonian transient solution of Szymanski (1932) added to the steady state Bingham solution. The rheology of the Bingham fluid is not present in the time-dependent portion of Atabek's solution. The comparison of the solution of Atabek with the closed form solution presented here is similar to the comparison with Duggins (1972). The normalized axial velocity results compared in table 2 show that Atabek's (1964) model at early time steps produces negative velocity values, which are physically impossible for the boundary conditions applied to the problem.

The solutions of the normalized axial velocity and the normalized shear stress are shown in figures 4 through 17. These results were evaluated at nondimensional times, including 0.025, 0.051, 0.077, 0.103, 0.129, 0.467, and steady state. The even-numbered figures represent the normalized axial velocity plotted on the ordinate and the normalized tube radius plotted on the abscissa. The odd-numbered figures contain the normalized shear stress plotted on the ordinate and the normalized tube radius plotted on the abscissa. The progression of the plugged flow interface in time toward the steady state value of 0.25 is seen in figures 4, 6, 8, 10, 12, 14, and 16. The initial nonlinear shear stress profile is shown in figures 5, 7, 9, 11, and 13. As time approaches infinity (σ = 1000), the shear stress profile becomes linear in figures 15 and 17. The nonlinear characteristics of the shear stress profiles are consistent with the results of Szymanski (1932), in

the case of the Newtonian fluids, and with the results of Duggins (1972). It has been found that Duggins' assumption, which states that the deviation from the parabolic velocity profile of the sheared fluid would have a minimal effect on the instantaneous mean velocity, is not valid

Table 2. Comparison of Solution of Atabek (1964) and the Closed Form Solution of the Commencement of Flow for a Bingham Fluid

Time (non-dim.)	Φ_{max}/Φ_{ave} Atabek	Φ_{max}/Φ_{ave} Closed Form	Difference % Δ	% Steady State Solution
0.0513	–0.161	0.639	125.0	38.0
0.1014	0.372	0.937	60.0	56.0
0.1510	0.749	1.136	34.0	67.5
0.2002	1.013	1.280	21.0	76.0
0.2995	1.331	1.464	9.0	87.0
0.4007	1.495	1.564	4.4	93.0
0.5034	1.582	1.619	2.3	96.0
0.7520	1.681	1.669	0.5	99.0
1.0	1.6786	1.6806	0.1	99.8
1000.0	1.6842	1.6842	0.0	100.0

5. CONCLUSIONS

A closed form solution to the commencement of flow for a Bingham plastic fluid in an axisymmetric cylindrical tube is presented. This analytical model has shown that past numerical and analytical treatments of non-Newtonian fluid applications have inaccurate velocity profiles, resulting in errors of up to 125 percent. The concern with the past models is that the region of extreme error is in the time-dependent portion of the solutions. The velocity and shear stress profiles predicted in the closed form solution presented here will provide the accuracy needed to analyze flows with small time durations that include impulse loads, such as the oscillating flow of blood in an artery.

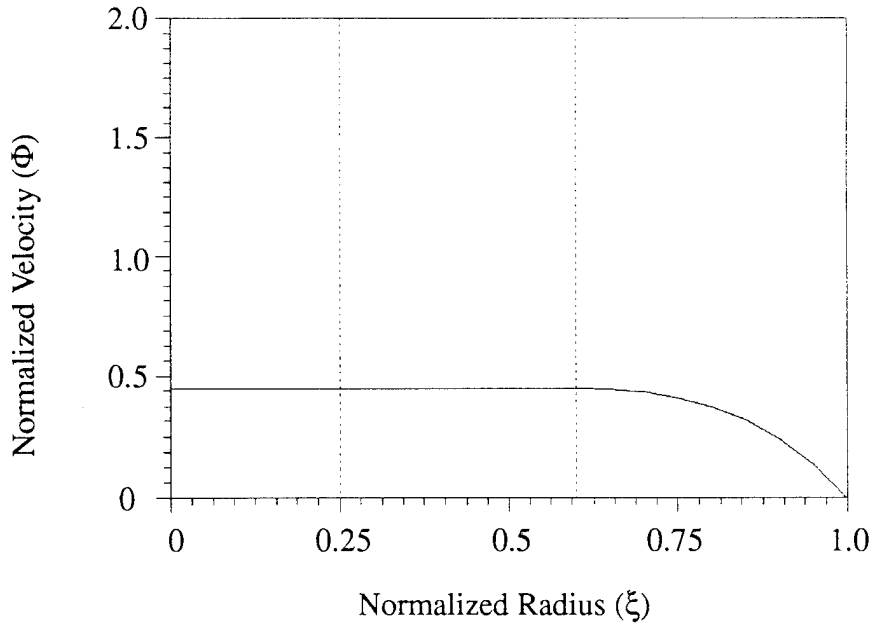

Figure 4. Axial Velocity Profile as a Function of Radial Location at 0.025 Nondimensional Time

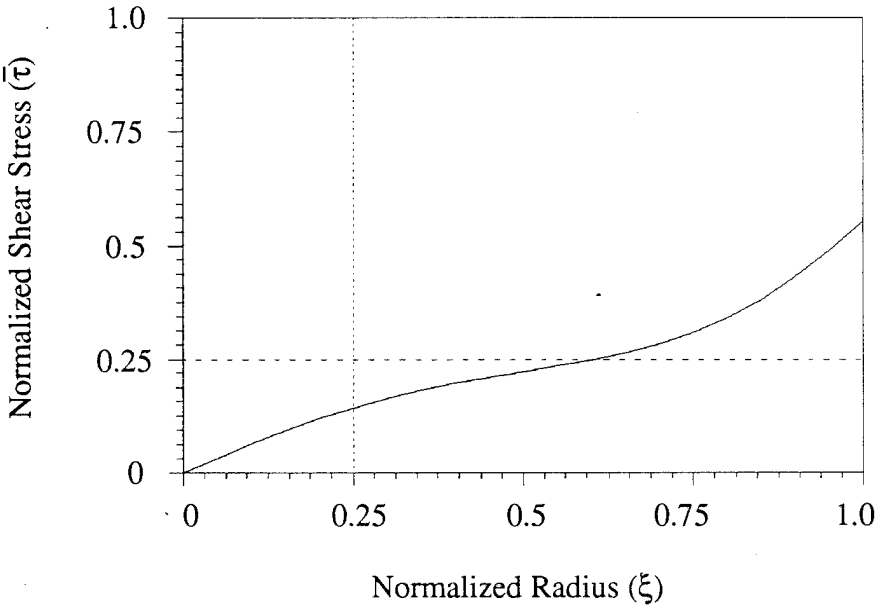

Figure 5. Shear Stress Profile as a Function of Radial Location at 0.025 Nondimensional Time

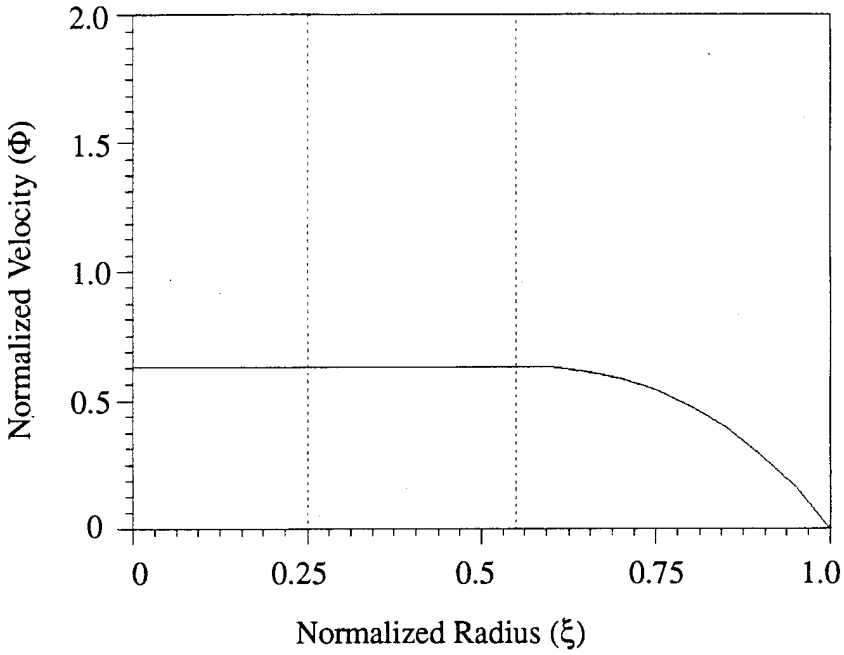

Figure 6. Axial Velocity Profile as a Function of Radial Location at 0.051 Nondimensional Time

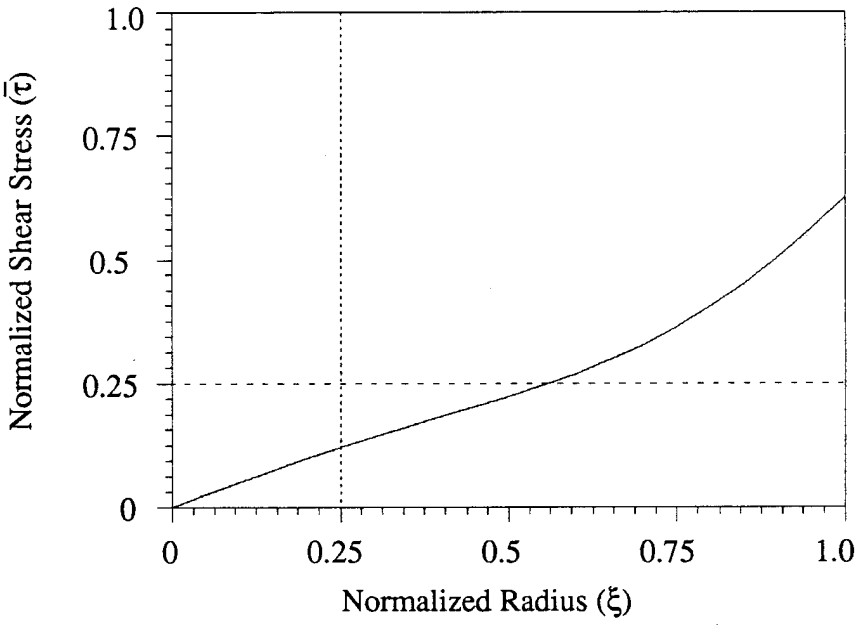

Figure 7. Shear Stress Profile as a Function of Radial Location at 0.051 Nondimensional Time

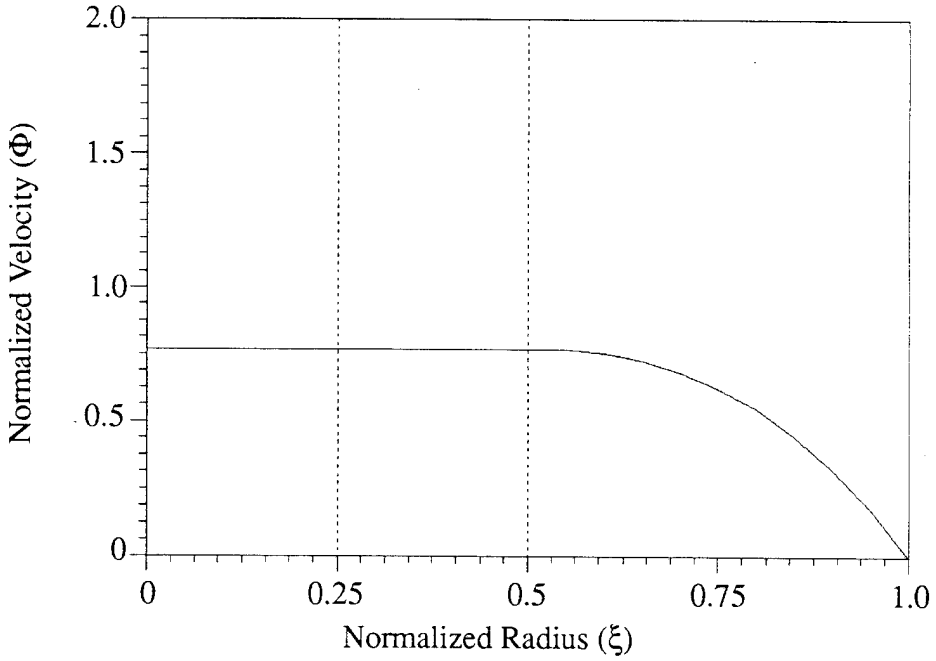

Figure 8. Axial Velocity Profile as a Function of Radial Location at 0.077 Nondimensional Time

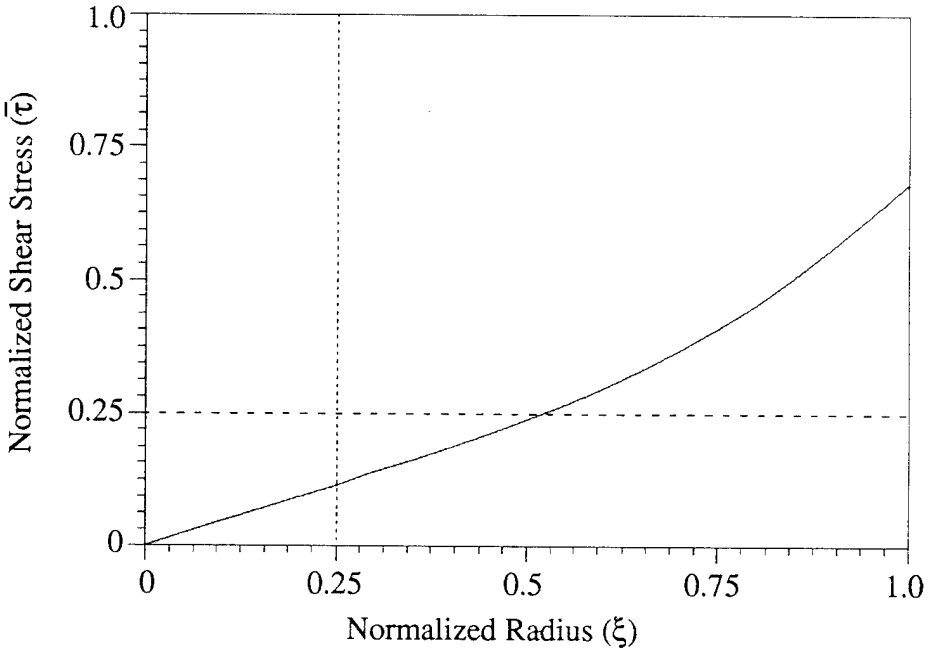

Figure 9. Shear Stress Profile as a Function of Radial Location at 0.077 Nondimensional Time

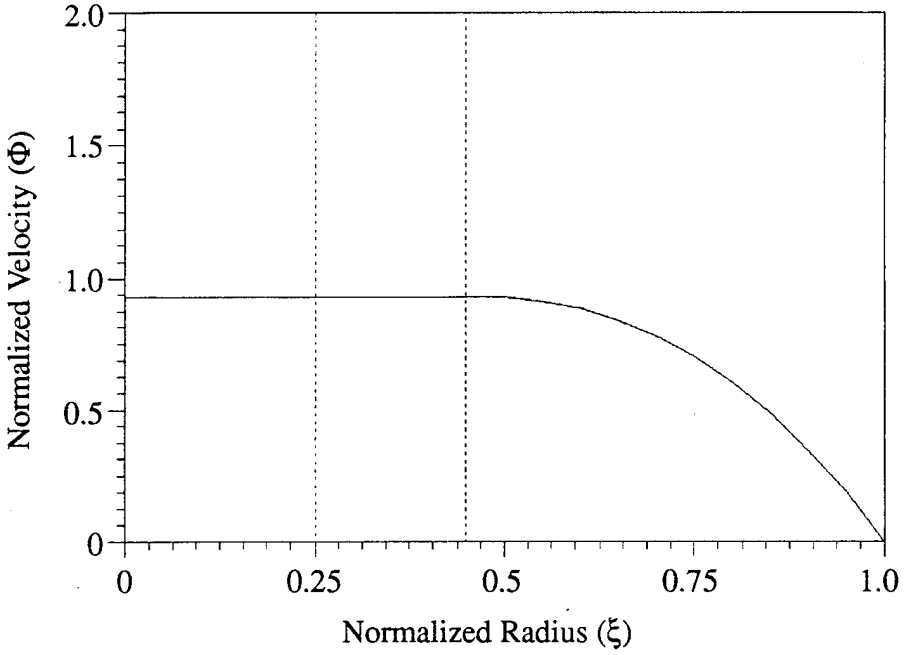

Figure 10. Axial Velocity Profile as a Function of Radial Location at 0.103 Nondimensional Time

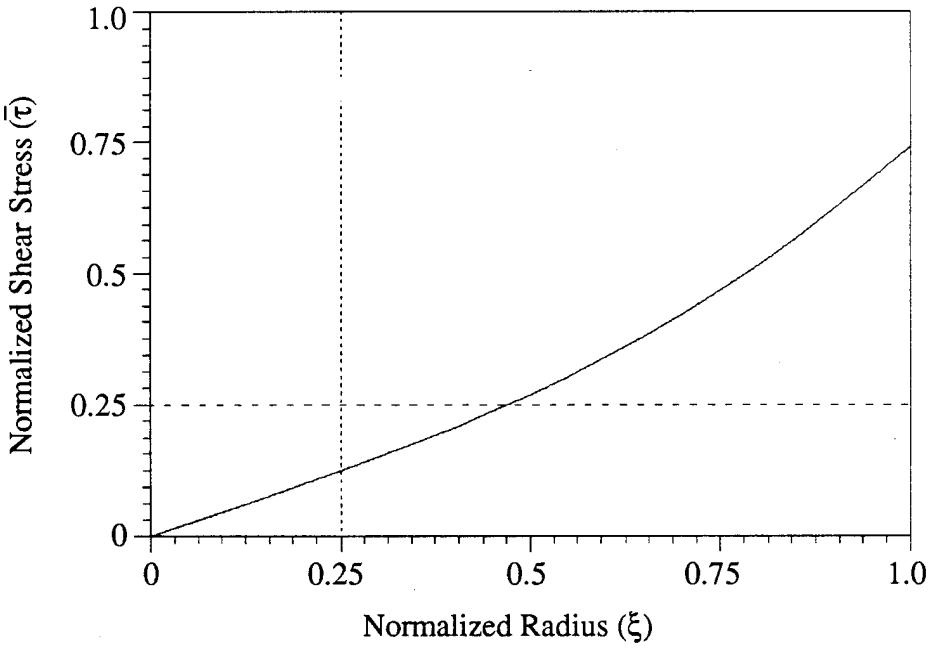

Figure 11. Shear Stress Profile as a Function of Radial Location at 0.103 Nondimensional Time

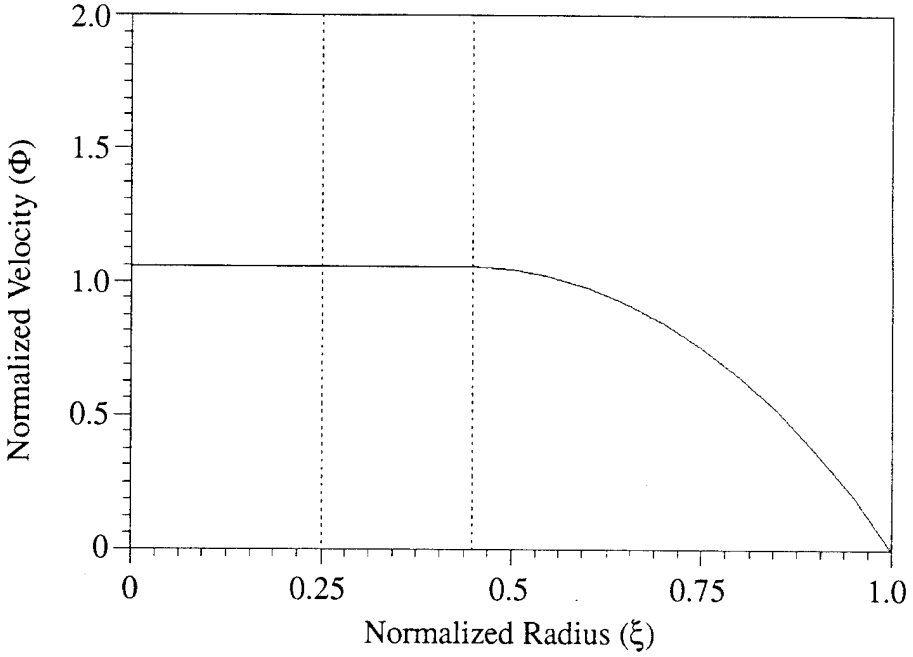

Figure 12. Axial Velocity Profile as a Function of Radial Location at 0.129 Nondimensional Time

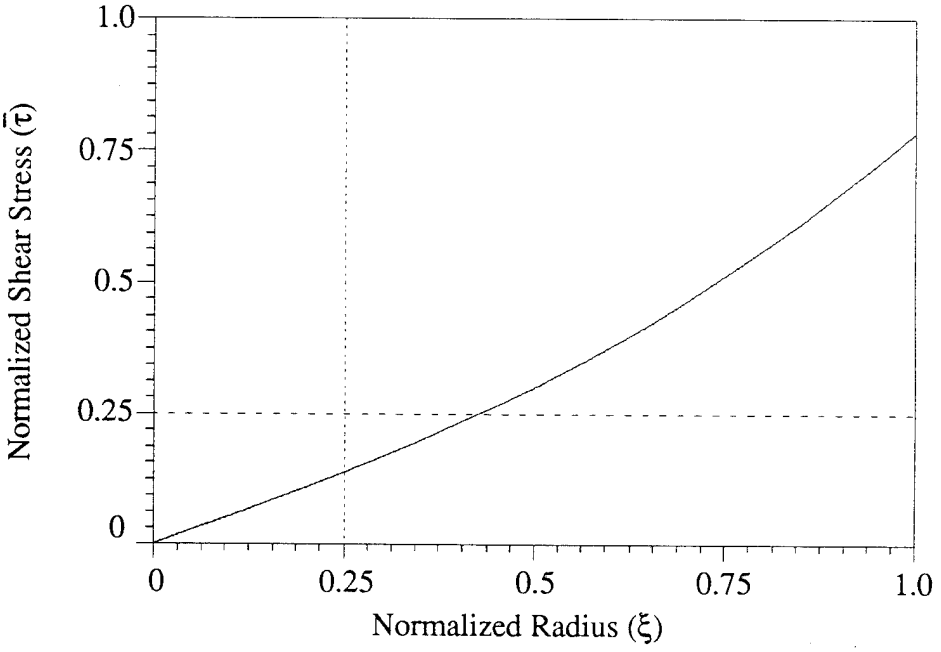

Figure 13. Shear Stress Profile as a Function of Radial Location at 0.129 Nondimensional Time

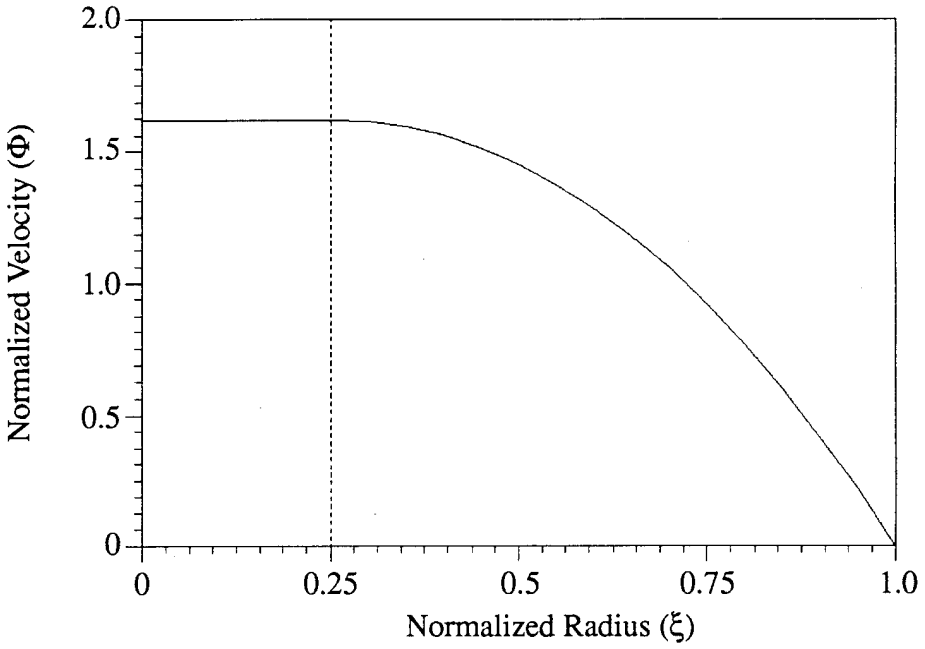

Figure 14. Axial Velocity Profile as a Function of Radial Location at 0.467 Nondimensional Time

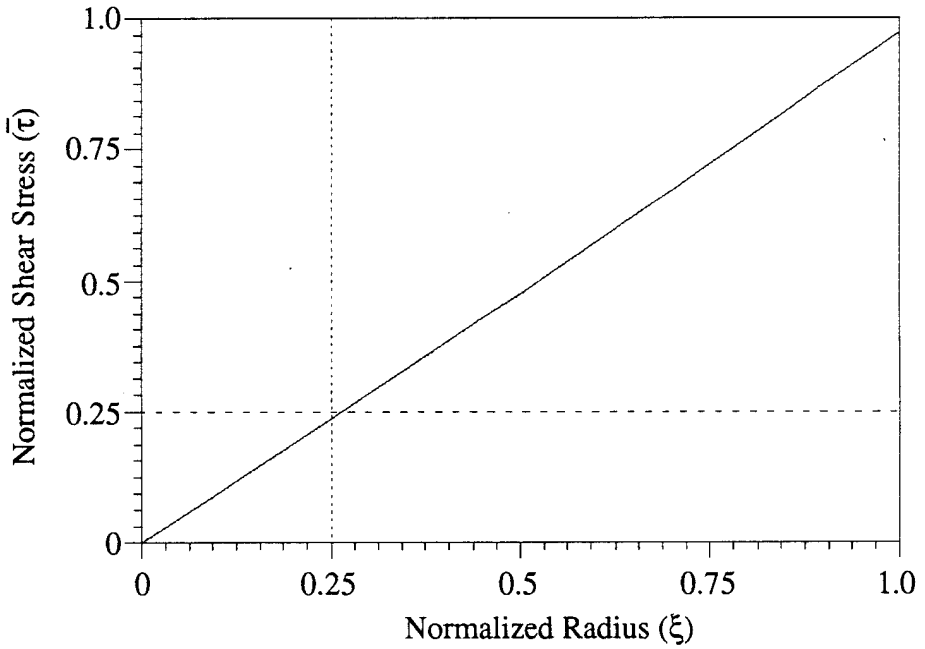

Figure 15. Shear Stress Profile as a Function of Radial Location at 0.467 Nondimensional Time

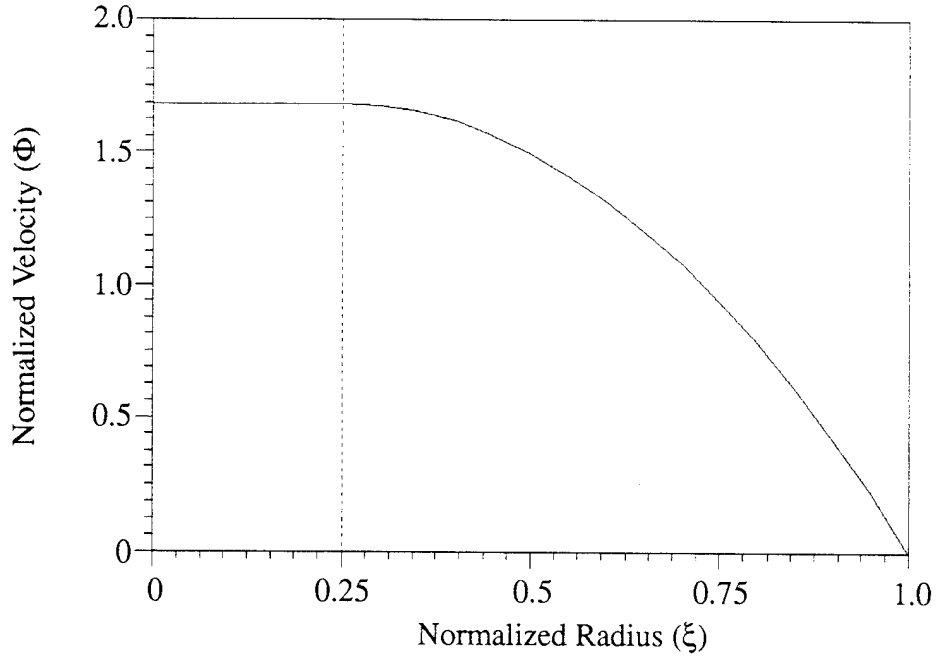

Figure 16. Axial Velocity Profile as a Function of Radial Location at Steady State

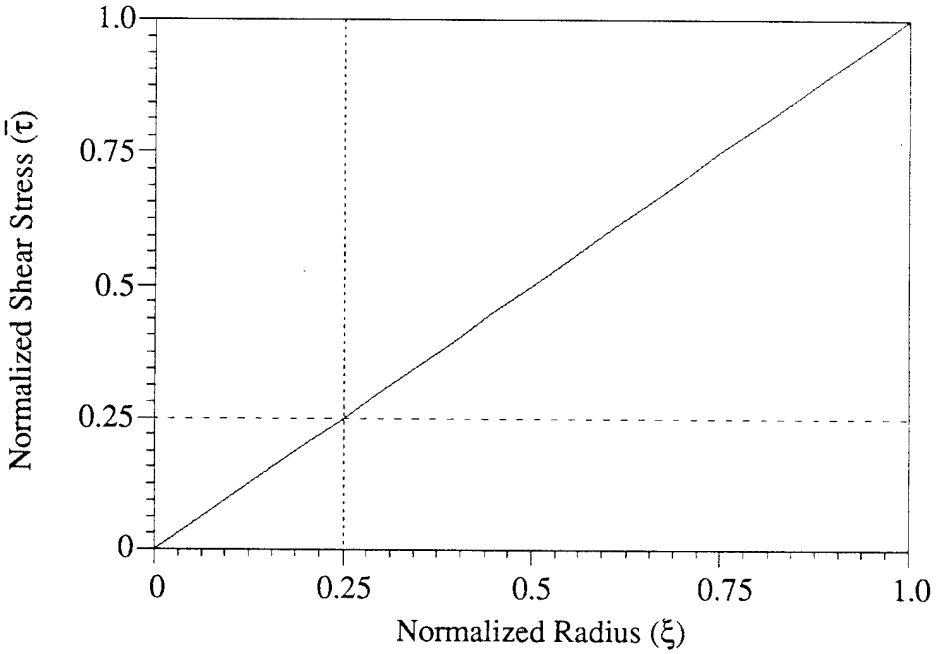

Figure 17. Shear Stress Profile as a Function of Radial Location at Steady State

6. REFERENCES

Atabek, H. B., 1964, "Start-Up Flow of a Bingham Plastic in a Circular Tube," *Kleine Mitteilungen*, vol. 44, pp. 332-333.

Atkin, R. J., Shi, X., and Bullough, W. A., 1991, "Solutions of the Constitutive Equations for the Flow of an Electrorheological Fluid in Radial Configurations," *Journal of Rheology,* vol. 35, pp. 1441-1461.

Bird, R. B., Stewart, W. E., and Lightfoot, E. N.,1960, *Transport Phenomena*, John Wiley & Sons, New York, NY.

Chen, S. S., Fan, L. T., and Hwang, C. L., 1970, *AIChE Journal*, vol. 16, p. 293.

Churchill, S. W., 1988, *Viscous Flows, The Practical Use of Theory*, Butterworth Publishing, Boston, MA.

Duggins, R. K., 1972, "The Commencement of Flow of a Bingham Plastic Fluid," *Chemical Engineering Science,* vol. 27, pp. 1991-1996.

Edwards, M. F., Nellist, D. A., and Wilkinson, W. L., 1972, "Unsteady Laminar Flows of Non-Newtonian Fluids in Pipes," *Chemical Engineering Science,* vol. 27, pp. 295-306.

Lipscomb, G. G., and Denn, M. M., 1984, "Flow of Bingham Fluids in Complex Geometries," *Journal of Non-Newtonian Fluid Mechanics,* vol. 14, pp. 337-346.

Potter, M. C., 1978, *Mathematical Methods in the Physical Sciences*, Prentice-Hall, Inc., New York, NY.

Szymanski, P. P., 1932, "L'Hydrodynamique du Fluide Visqueux," *J. Math. Pures Appliquees*, series 9, vol. 11, pp. 67-107.

Walton, I. C., and Bittleson, S. H., 1991, "The Axial Flow of a Bingham Plastic in a Narrow Eccentric Annulus," *Journal of Fluid Mechanics,* vol. 222, pp. 39-60.

INITIAL DISTRIBUTION LIST

Addressee	No. of Copies
Defense Technical Information Center	12
University of Connecticut (Professor L. S. Langston, Professor J. C. Bennett)	2
University of Hartford (Professor F. Lahey)	1
Office of Naval Research (K. W. Ng (Code 452B4)	1